Projected surface energy bands of bcc iron*

Ed Caruthers and Leonard Kleinman
Department of Physics, The University of Texas, Austin, Texas 78712
(Received 21 January 1974)

We have projected Wood's calculated three-dimensional energy bands of paramagnetic iron to obtain band gaps in the two-dimensional energy bands for (001) and (110) paramagnetic iron surfaces. Extensive band gaps show the possibitlity that many surface states exist. The most important surface states probably exist well away from the center of the two-dimensional Brillouin zone, and may explain the existence of magnetically dead layers at surfaces of Fe and Ni.

In our work on aluminum[1-3] we developed a method of projecting the bulk part of the two-dimensional band structure. In this method, we form a unit cell in reciprocal space having the same base as the two-dimensional Brillouin zone (2D BZ). The height $2K_3$ of this cell is taken to be that which gives the same volume as the three-dimensional (3D) BZ. This unit cell we call an extended slab-adapted BZ. The allowed energies at a point $\bar{k}$ in the 2D BZ are then the eigenvalues at all the points $(\bar{k}, k_3)$ such that $-K_3 \leq k_3 \leq K_3$. (If we consider a slab with reflection symmetry parallel to the surface, then we need only sample $0 \leq k_3 \leq K_3$.) This method of projection gives continua of states at $\bar{k}$ with symmetries corresponding to the symmetries along the lines from $(\bar{k}, -K_3)$ to $(\bar{k}, K_3)$. Surface states can exist only for values of $\bar{k}$ and E at which gaps appear. Such states do not go over into bulk states as we go to infinitely thick slabs. They are characterized by complex values of the normal component of their wave vectors, such that they decay on moving into the film.

An example of this process is shown in Fig. 1. The continua of various symmetries at the $\bar{\Gamma}$ point in the (100) face of tungsten are projected from the Δ lines in three dimensions. These 3D bands are taken from Louck's relativistic calculation.[4] The gap in Δ_7 levels at an energy of about 0.9 Ry results from spin-orbit coupling. Though it is completely filled by states of Δ_6 symmetry, a surface state of Δ_7 symmetry can still exist within this subband gap. In fact, observed surface states in W (Ref. 5–7) have been attributed to this gap.[8-10] To carry this example a step further, note that as we move away from $\bar{\Gamma}$ along a general direction in the 2D BZ the difference in symmetry between Δ_6 and Δ_7 is lost. There is no gap of any kind and no surface states can exist. But since a single point in the BZ is of zero measure and cannot be observed experimentally, what is observed is either surface resonances from the region around $\bar{\Gamma}$ or surface states from some other region of the BZ. This simple example demonstrates the utility of projected energy bands.

In previous work we have used this method to locate both absolute and subband gaps. Subsequent thin-film calculations showed surface states in all gaps and prompted us to speculate that this may be a general result in nearly-free-electron (NFE) metals. At the same time, Gurman and Pendry[11] have examined d-band metals analytically. They concluded that a gap has a 50% chance of being occupied if it results from band splitting at a 3D-zone boundary and a 70% chance of being occupied if it results from hybridization away from a zone boundary. We have therefore projected bands for the (001) and (110) bands of nonmagnetic bcc Fe. We present these results here in the expectation that our more detailed thin-film calculations will show that most band gaps are filled. This expectation is reinforced by the finding of surface states in two gaps at $\bar{\Gamma}$ in the (110) face by Tomášek and Mikušík.[12] Most work on surface states has concentrated on the $\bar{\Gamma}$ point,[12-14] and another reason for presenting these bands is to show that surface states at other points in the BZ probably have more important physical effects than those at $\bar{\Gamma}$.

We have projected 2D bands from the 3D bands of Wood,[15] shifting his zero of energy to obtain the correct work functions of 4.7 eV.[16] These results were presented (complete with symmetry labeling) at 55 points within the irreducible wedge of the bcc BZ. This corresponds to a cubic mesh produced by dividing each fourfold axis into eighths. The points in this cubic mesh were commensurate with the (001) and (110) 2D BZ's, and the mesh size was small enough for projection of many $2D$ points. Though these results were derived for nonmagnetic (β-phase) Fe, it is expected that the magnetic phase (α-Fe) can be reasonably represented by rigid shifts in the bands. The self-consistent calculation by Tawil and Callaway[17] shows spin-up–versus–spin-down

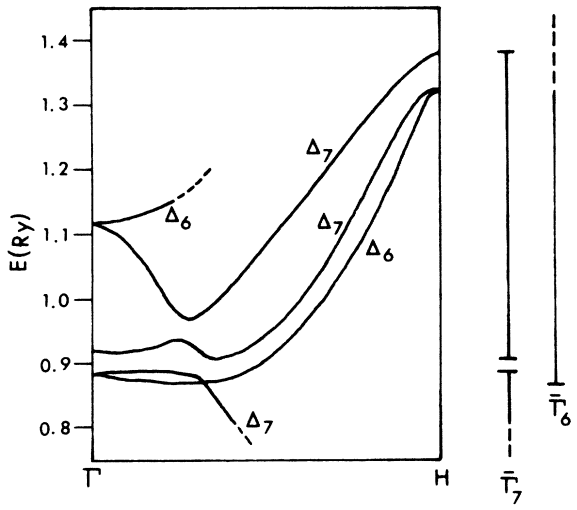

FIG. 1. Relativistic energy bands for tungsten along the [100] direction.

shifts averaging 0.165 Ry for d-like levels. The smallest shift in such a level was 0.128 Ry and the largest was 0.185 Ry.

Figure 2 shows the crystal structures and BZ's for (001) and (110) oriented thin films of any bcc material. The labeling of the high-symmetry lines and points is consistent with that used for the surface phonon problem.[18] For the (001) face, the 2D lattice vectors are $\vec{a} = a\hat{x}$, $\vec{b} = a\hat{y}$, where a is the edge length of the 3D cube, and $\hat{x}$, $\hat{y}$, $\hat{z}$ are the usual 3D unit vectors. The reciprocal lattice vectors are $\vec{K}_1 = (2\pi/a)\hat{x}$ and $\vec{K}_2 = (2\pi/a)\hat{y}$. To make the volume of the extended slab-adapted BZ the same as that of the primitive bcc BZ, we must have $\vec{K}_3 = (2\pi/a)\hat{z}$. Since there is reflection symmetry that takes $\hat{z}$ into $-\hat{z}$, we need only sample $k_3 = (2\pi/a)k_z$ from $0 \leq k_z \leq 1$. In terms of the usual 3D vectors $(k_x, k_y, k_z) = (2\pi/a)(k_x\hat{x} + k_y\hat{y} + k_z\hat{z})$, the (001) $\bar{\Gamma}$ point is projected from the 3D line $(0, 0, k_z)$. The $\bar{\Delta}$ line is projected from the lines $(k_x, 0, k_z)$, $0 \leq k_x \leq \frac{1}{2}$. The $\bar{X}$ point is projected from the line $(\frac{1}{2}, 0, k_z)$. The $\bar{Y}$ line is projected from the lines $(\frac{1}{2}, k_y, k_z)$, $0 \leq k_y \leq \frac{1}{2}$. The $\bar{M}$ point is projected from the line $(\frac{1}{2}, \frac{1}{2}, k_z)$, and the $\bar{\Sigma}$ line is projected from the lines (k_x, k_y, k_z), $\frac{1}{2} \geq k_x = k_y \geq 0$.

For the (110) face, the lattice vectors are given by $\vec{a} = \frac{1}{2}a(-\hat{x} + \hat{y} - \hat{z})$ and $\vec{b} = \frac{1}{2}a(-\hat{x} + \hat{y} + \hat{z})$. The reciprocal lattice vectors are $\vec{K}_1 = (\pi/a)(-\hat{x} + \hat{y} - 2\hat{z})$ and $\vec{K}_2 = (\pi/a)(-\hat{x} + \hat{y} + 2\hat{z})$. The directions of the rectangular axes $\tilde{x}$ and $\tilde{y}$ are $-\hat{z}$ and $-\hat{x} + \hat{y}$, respectively. $\vec{K}_3 = (\pi/a)(\hat{x} + \hat{y})$, but again there is reflection symmetry, taking $\hat{x} + \hat{y}$ into $-\hat{x} - \hat{y}$, so we only sample $\vec{k}_3 = (2\pi/a)(\gamma, \gamma, 0)$, $0 \leq \gamma \leq \frac{1}{2}$, for any 2D point. The $\bar{\Gamma}$ point is projected from $(\gamma, \gamma, 0)$. The $\bar{\Sigma}$ line is projected from (γ, γ, α), $0 \geq \alpha \geq -\frac{3}{4}$. The $\bar{D}$ line is projected from $(\gamma - \alpha, \gamma + \alpha, -\frac{3}{4} + \alpha)$, $0 \leq \alpha \leq \frac{1}{2}$. The $\bar{S}$ point is projected from $(\gamma - \frac{1}{4}, \gamma + \frac{1}{4}, -\frac{1}{2})$. The $\bar{C}$ line is projected from $(\gamma - \frac{1}{2}, \gamma + \frac{1}{2}, -\frac{1}{4} + \alpha)$, $0 \leq \alpha \leq \frac{1}{4}$. The $\bar{Y}$ point is projected from $(\gamma - \frac{1}{2}, \gamma + \frac{1}{2}, 0)$, and the $\bar{\Delta}$ line is projected from $(-\alpha + \gamma, \alpha + \gamma, 0)$, $\frac{1}{2} \geq \alpha \geq 0$. Finally, the $\bar{\Lambda}$ line is projected from $(\gamma - \alpha, \gamma + \alpha, -2\alpha)$, $0 \leq \alpha \leq \frac{1}{4}$.

The projected energy bands for the (001) and (110) faces of β-Fe are shown in Figs. 3 and 4, respectively. Before going into details about the origins of the various gaps, a few general comments are appropriate. First, there are many more band gaps than in the NFE materials pre-

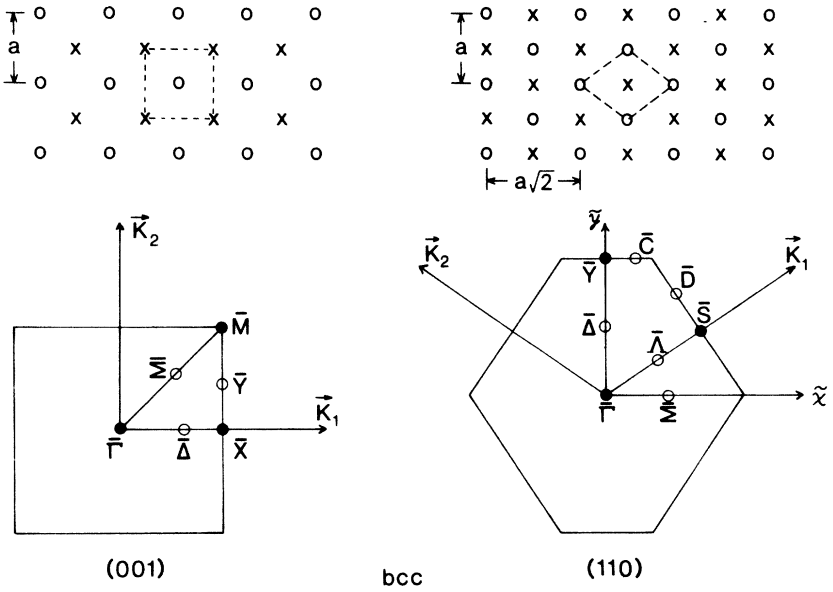

FIG. 2. Crystal structures and Brillouin zones for the (001) and (110) faces of bcc Fe.

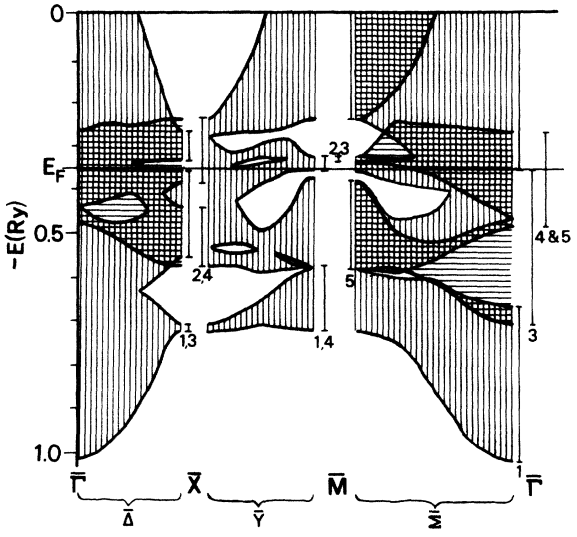

FIG. 3. Projected two-dimensional energy bands for the (001) face of bcc Fe.

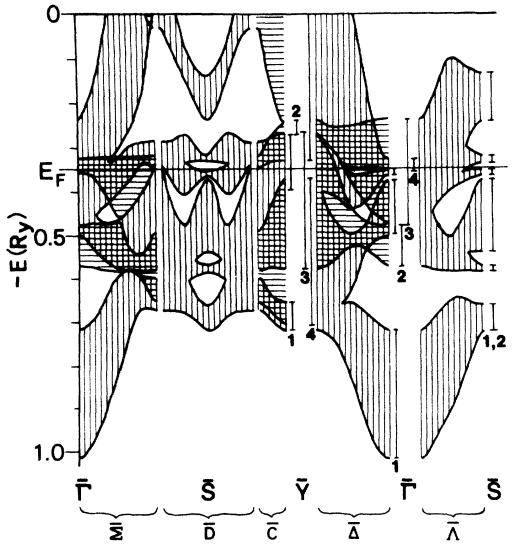

FIG. 4. Projected 2D energy bands for the (110) face of bcc Fe.

viously studied,[1,2,3,19,20] and the gaps are more complicated. In the Al and Li calculations the gaps were always widest at high-symmetry points, and narrowed going away from them. Here we see gaps of this type, but we also see gaps which widen as they go away from symmetry points, or which pinch off before they ever reach the high-symmetry points. Of course transition metals have more complicated bands than NFE metals, even in 3D. But one might expect the increased density of *d* bands to make overlap more common and gaps less likely. Obviously, this is not the case. Second, those gaps which are closest to the Fermi level and thus likely to be of greatest physical importance are located well away from $\bar{\Gamma}$. As mentioned above, most work on surface states has focused on the $\bar{\Gamma}$ points. We think that this emphasis is misplaced and that attempts to explain physical properties—e.g., surface magnetic dead layers[21,22]—in terms of $\bar{\Gamma}$ surface states will be unsuccessful.

TABLE I. Connectivity relations for the points and lines of high symmetry in the Brillouin zone of (001) bcc iron.

$$\bar{\Gamma}_1, \bar{\Gamma}_3 \leftrightarrow \bar{\Delta}_1 \leftrightarrow \bar{X}_1, \bar{X}_3$$
$$\bar{\Gamma}_2, \bar{\Gamma}_4 \leftrightarrow \bar{\Delta}_2 \leftrightarrow \bar{X}_2, \bar{X}_4$$
$$\bar{\Gamma}_5 \leftrightarrow \bar{\Delta}_1, \bar{\Delta}_2$$

$$\bar{\Gamma}_1, \bar{\Gamma}_4 \leftrightarrow \bar{\Sigma}_1 \leftrightarrow \bar{M}_1, \bar{M}_4$$
$$\bar{\Gamma}_2, \bar{\Gamma}_3 \leftrightarrow \bar{\Sigma}_2 \leftrightarrow \bar{M}_2, \bar{M}_3$$
$$\bar{\Gamma}_5 \leftrightarrow \bar{\Sigma}_1, \bar{\Sigma}_2 \leftrightarrow \bar{M}_5$$

$$\bar{M}_1, \bar{M}_3 \leftrightarrow \bar{Y}_1 \leftrightarrow \bar{X}_1, \bar{X}_2$$
$$\bar{M}_2, \bar{M}_4 \leftrightarrow \bar{Y}_2 \leftrightarrow \bar{X}_3, \bar{X}_4$$
$$\bar{M}_5 \leftrightarrow \bar{Y}_1, \bar{Y}_2$$

In Fig. 3 vertical crosshatching is used to show the extent of $\bar{\Delta}_1$, $\bar{Y}_{1,2}$, and $\bar{\Sigma}_1$ states. Horizontal crosshatching is used to show the extent of $\bar{\Delta}_2$ and $\bar{\Sigma}_2$ states. At $\bar{\Gamma}$, $\bar{X}$, and $\bar{M}$ there are more symmetries and their extents are indicated separately. Table I shows the 2D connectivities. Our $\bar{\Gamma}_1$ line comes from Wood's Δ_1 line in 3D. Our $\bar{\Gamma}_3$ comes from his Δ_2 line, our $\bar{\Gamma}_4$ from his Δ_2 line, and our $\bar{\Gamma}_5$ from his Δ_5. There is a wide gap in $\bar{\Gamma}_1$ states, part of which persists as a gap in $\bar{\Sigma}_1$ states. But this gap does not persist at all in the $\bar{\Delta}$ direction, or in any general direction, so that its contribution to the surface density of states is of zero measure.

There is one gap along $\bar{\Delta}$ which does not exist at either $\bar{\Gamma}$ or $\bar{X}$. It is a gap in $\bar{\Delta}_1$ states which connect to $\bar{\Gamma}_3$ and $\bar{\Gamma}_5$ states. Since the symmetries are different at $\bar{\Gamma}$, the $\bar{\Gamma}_3$ and $\bar{\Gamma}_5$ lines can cross, and the gap is pinched off. This $\bar{\Delta}_1$ gap becomes indirect and pinches off before reaching $\bar{X}$ because two lines of the same symmetry overlap. Figure 5 shows the 3D lines which are projected back to form the $\bar{\Delta}(\frac{3}{8}, 0)$ point. The overlap between the second and third $\bar{\Delta}_1$ lines goes away as we move toward $\bar{\Gamma}$, producing the gap just discussed. The gap between the first and second $\bar{\Delta}_1$ lines increases as we go toward $\bar{X}$, and becomes an overlap as we go toward $\bar{\Gamma}$. The same happens to the gap between the third and fourth $\bar{\Delta}_1$ lines. We can also see a minimal overlap between the

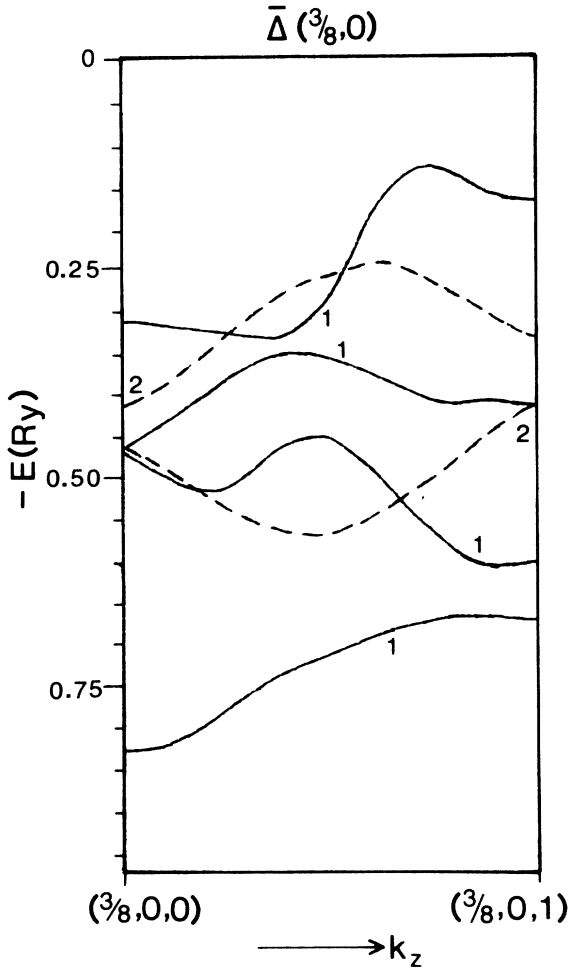

FIG. 5. Three-dimensional energy bands from which energy levels at the $\bar{\Delta}$ ($\frac{3}{8}$, 0) point of the (001) face are projected.

two $\bar{\Delta}_2$ states. This becomes greater as we go toward $\bar{\Gamma}$, but in moving toward $\bar{X}$ the overlap is lost and a gap develops.

All levels along $\bar{Y}$, from $\bar{X}$ to $\bar{M}$ are twofold degenerate because the 3D points $(\frac{1}{2}, y, z)$ and $(\frac{1}{2}, y, 1-z) = (-\frac{1}{2}, y, -z)$ go into one another under the twofold rotation about the y axis. Thus the only gap which persists in going from $\bar{X}$ toward $\bar{M}$ is the absolute gap caused by part of the lowest $\bar{X}_{1,3}$ gap lying below the $\bar{X}_{2,4}$ continuum. The lower absolute gap at $\bar{M}$ is between $k_z = 0$ states and comes from the N_1–$N_{1'}$ gap in 3D. Moving toward $\bar{X}$, this gap widens until it becomes an indirect gap between $k_z = 0$ on the upper curve and $k_z = \frac{1}{2}$ on the lower curve. The gap finally pinches off as the $k_z = 0$ and $k_z = \frac{1}{2}$ levels overlap. The upper absolute gap at $\bar{M}$ comes from the N_3–N_4 gap in 3D. This narrows in the $\bar{Y}$ direction, then becomes an indirect gap and widens out again. It

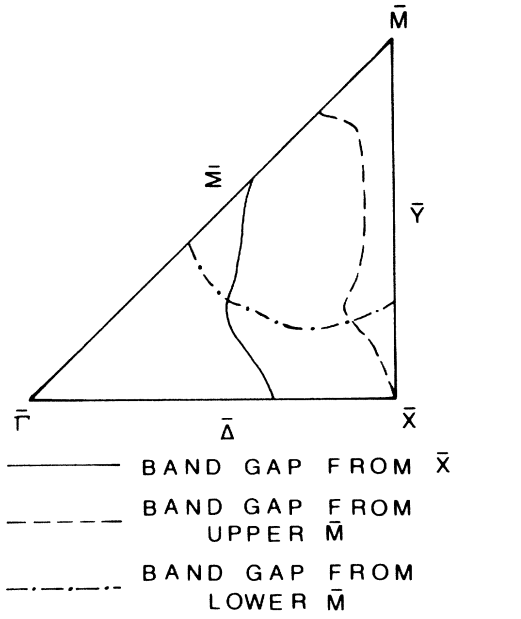

FIG. 6. Extents of the three major absolute gaps in the (001) projected bands.

finally pinches off at $\bar{X}$ as the two bands go to lines of different symmetry which cross. There are three gaps along $\bar{Y}$ which exist at neither $\bar{M}$ nor $\bar{X}$. Each is narrow and indirect, except that at its widest point the uppermost gap becomes direct. The extent of each gap will therefore depend greatly on the details of the potential used in calculating the 3D energy bands.

As we move from $\bar{M}$ toward $\bar{\Gamma}$, the highest $\bar{\Sigma}_2$ level moves upward into the vacuum until there is a wide gap between the highest $\bar{\Gamma}_5$ level and the vacuum. The lower $\bar{\Sigma}_2$ gap is indirect, but widens considerably in going away from $\bar{M}$. It finally pinches off when $\bar{\Gamma}_5$ and $\bar{\Gamma}_3$ levels cross at about $(0, 0, \frac{1}{4})$ in 3D. The upper $\bar{\Sigma}_1$ gap at $\bar{M}$ becomes indirect and pinches off about 38% of the way to $\bar{\Gamma}$. The absolute gap extends only about 19% of the way from $\bar{M}$ to $\bar{\Gamma}$. The lower $\bar{\Sigma}_1$ gap from $\bar{M}$ becomes indirect, then widens as it becomes direct, and finally becomes indirect and pinches off about 60% of the way to $\bar{\Gamma}$. Since it is wholly contained within the $\bar{\Sigma}_2$ gap, we again have an absolute gap of considerable size. In Fig. 6 we show the extent of this absolute gap through the 2D BZ, as well as the extents of the other two major absolute gaps.[23]

The projected bands for (110) β-Fe are still more complicated. In Fig. 4 we show the extent of $\bar{\Sigma}_1$, $\bar{C}_1$, and $\bar{\Delta}_1$ states with vertical crosshatching. We show the extent of $\bar{\Sigma}_2$, $\bar{C}_2$, and $\bar{\Delta}_2$ states with horizontal crosshatching. At $\bar{\Gamma}$ and $\bar{Y}$ there are more than two symmetries, so the

TABLE II. Connectivity relations for the points and lines of high symmetry in the Brillouin zone of (110) bcc Fe.

$\bar{\Gamma}_1, \bar{\Gamma}_3 \leftrightarrow \bar{\Sigma}_1 \leftrightarrow \bar{D}_1$
$\bar{\Gamma}_2, \bar{\Gamma}_4 \leftrightarrow \bar{\Sigma}_2 \leftrightarrow \bar{D}_1$
$\bar{D}_1 \leftrightarrow \bar{C}_1 \leftrightarrow \bar{Y}_1, \bar{Y}_3$
$\bar{D}_1 \leftrightarrow \bar{C}_2 \leftrightarrow \bar{Y}_4, \bar{Y}_2$
$\bar{Y}_1, \bar{Y}_4 \leftrightarrow \bar{\Delta}_1 \leftrightarrow \bar{\Gamma}_1, \bar{\Gamma}_4 \leftrightarrow \bar{\Lambda}_1$
$\bar{Y}_2, \bar{Y}_3 \leftrightarrow \bar{\Delta}_2 \leftrightarrow \bar{\Gamma}_2, \bar{\Gamma}_3 \leftrightarrow \bar{\Lambda}_1$
$\bar{D}_1 \leftrightarrow \bar{S}_1, \bar{S}_2 \leftrightarrow \bar{\Lambda}_1$

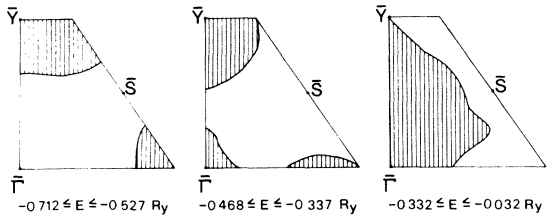

FIG. 7. Extents of the three major absolute gaps in the (110) projected bands. The gaps are represented by the unshaded regions.

extent of the various continua are indicated separately. Along $\bar{D}$ and $\bar{\Lambda}$ all states are of a single symmetry. Vertical crosshatching is used to show continua along these lines. At $\bar{S}$ all levels are $\bar{S}_1$, $\bar{S}_2$ degenerate. The connectivity relations for the (110) bcc BZ are shown in Table II. The absolute gaps and subband gaps arise in the same way that they do in the (001) face. There are again three absolute gaps which exist over large regions of the 2D BZ. The lowest exists at $\bar{\Gamma}$, extends about threefourths of the way along both the $\bar{\Sigma}$ and $\bar{\Delta}$ directions, extends all the way to $\bar{S}$, and extends from $\bar{S}$ along $\bar{D}$ in both directions. This gap exists in the energy range -0.712 Ry $\leq E \leq -0.527$ Ry. The next important gap exists along short portions of $\bar{\Sigma}$ and $\bar{\Delta}$, along most of $\bar{\Lambda}$, and along all of $\bar{D}$ except its endpoints. This gap is narrow at $\bar{S}$, and only a few hundredths of a Ry below E_F. Going away from $\bar{S}$, the gap drops to lower energy and widens. Surface states in this gap would have energies between -0.468 and -0.337 Ry. The third gap is somewhat wider at $\bar{S}$, becomes much wider by the time it reaches the end of the $\bar{D}$ line, then pinches off along the $\bar{\Sigma}$ and $\bar{C}$ lines. It extends only a little way from $\bar{S}$ along $\bar{\Lambda}$ and does not exist at $\bar{\Gamma}$. This gap exists in the energy range $-0.332 \leq E \leq -0.032$ Ry. Two additional absolute gaps exist at $\bar{S}$, but they are narrow and pinch off quickly in either the $\bar{D}$ or $\bar{\Lambda}$ direction. Figure 7 shows the extent of the three most important absolute gaps.

Of course, surface states can exist in subband gaps, but these gaps do not persist along general directions in the 2D BZ. Along such directions the surface states become surface resonances (states which propagate uniformly into the bulk, but have a maximum at the surface). Such resonances will contribute to the surface density of states and therefore to the results of experiments such as field emission[10] and photoemission but to a lesser extent than would surface states.

The presence of extensive absolute gaps very near E_F suggests an explanation for the surface magnetic dead layers observed in α-Fe.[22] In Li and Al we found that surface states within gaps caused antisurface states (i.e., states which because of their orthogonality to the surface states are of small amplitude near the surface) at the edges of the gaps. If there are surface states in the gaps immediately above and below the paramagnetic Fermi level, then the peak in density of states occuring near E_F will translate to a much reduced peak in the surface density of states. Furthermore, in order to maintain charge neutrality at the surface, the surface density of states curve will have to drop in energy causing E_F to occur on the high-energy wing of this reduced peak of the surface density of states, thus giving a further lowering of the surface density of states at E_F. If the surface density of states is low enough, then the paramagnetic phase may be stabilized at the surface. Of course, it is possible, if the surface states in the gaps above E_F lie close enough to E_F, that the ferromagnetic state would be stable even at the surface, and that the surface states would be occupied by majority spins. Only more detailed calculations can determine the actual situation. But we would like to point out that in both Fe and Ni the paramagnetic E_F lies on a peak in the density of states. This peak comes from flat $3d$ bands so that there are necessarily gaps in the projected energy bands nearby. So this possible mechanism for surface magnetic dead layers arises in a natural way from the nature of surface states and the nature of the paramagnetic-ferromagnetic transition.

*Work supported by the National Science Foundation under Grant No. GH-40371.

[1]E. B. Caruthers, L. Kleinman, and G. P. Alldredge, Phys. Rev. B 8, 4570 (1973).
[2]E. B. Caruthers, L. Kleinman, and G. P. Alldredge Phys. Rev. B 9, 3325 (1974).
[3]E. B. Caruthers, L. Kleinman, and G. P. Alldredge Phys. Rev. B 9, 3330 (1974).
[4]T. L. Loucks, Phys. Rev. Lett. 14, 693 (1965).
[5]E. W. Plummer and R. W. Young, Phys. Rev. B 1, 2088 (1970).
[6]B. J. Waclawski and E. W. Plummer, Phys. Rev. Lett. 29, 783 (1972).
[7]B. Feuerbacher and B. Fitton, Phys. Rev. Lett. 29, 786 (1972).
[8]E. W. Plummer and J. W. Gadzuk, Phys. Rev. Lett. 25, 1493 (1970).
[9]C. Lea and R. Gomer, J. Chem. Phys. 54, 3349 (1971).
[10]J. W. Gadzuk, J. Vac. Sci. Technol. 1, 590 (1972).
[11]S. J. Gurman and J. B. Pendry, Phys. Rev. Lett. 31, 637 (1973).
[12]M. Tomášek and P. Mikušík, Phys. Rev. B 8, 410 (1973).
[13]F. Forstman and V. Heine, Phys. Rev. Lett. 24, 1419 (1970).
[14]F. Forstman and J. B. Pendry, Z. Phys. 235, 75 (1970).
[15]J. H. Wood, Phys. Rev. 126, 517 (1962).
[16]A. B. Cardwell, Phys. Rev. 92, 554 (1953).
[17]R. A. Tawil and J. Callaway, Phys. Rev. B 7, 4242 (1973).
[18]R. E. Allen, G. P. Alldredge, and F. W. de Wette, Phys. Rev. B 4, 1648 (1971).
[19]G. P. Alldredge and L. Kleinman, Phys. Rev. Lett. 28, 1264 (1972).
[20]G. P. Alldredge and L. Kleinman, Phys. Rev. B (to be published).
[21]L. Lieberman, J. Clinton, D. Edwards, and J. Mathon, Phys. Rev. Lett. 25, 232 (1970).
[22]L. Lieberman, D. Fredkin, and H. Shore, Phys. Rev. Lett. 22, 539 (1969).
[23]We show the gap around $\bar{X}$ extending to the $\bar{\Sigma}$ line. There is a narrow gap (see Fig. 3) which pinches off at $\bar{M}$ as does the $\bar{Y}$ gap. These appear to be parts of the same gap, but we do not have a dense enough sampling of the 3D energy bands to be certain that there are not regions near $\bar{M}$ where the gap disappears.